

Damping of relativistic electron beams by synchrotron radiation

F. Andersson, P. Helander, and L.-G. Eriksson

Citation: *Phys. Plasmas* **8**, 5221 (2001); doi: 10.1063/1.1418242

View online: <http://dx.doi.org/10.1063/1.1418242>

View Table of Contents: <http://pop.aip.org/resource/1/PHPAEN/v8/i12>

Published by the [American Institute of Physics](#).

Related Articles

Study of nonlinear interaction between bunched beam and intermediate cavities in a relativistic klystron amplifier
Phys. Plasmas **19**, 073104 (2012)

Acceleration of electrons to high energies in a standing wave generated by counterpropagating intense laser pulses with tilted amplitude fronts
Phys. Plasmas **19**, 073102 (2012)

Smooth magnetic cusp profile calculation for axis-encircling electron beam generation
Phys. Plasmas **19**, 043102 (2012)

Free electron terahertz wave radiation source with two-section periodical waveguide structures
J. Appl. Phys. **111**, 063107 (2012)

Gain in two stream free electron laser with planar wiggler and ion-channel guiding
Phys. Plasmas **19**, 023115 (2012)

Additional information on Phys. Plasmas

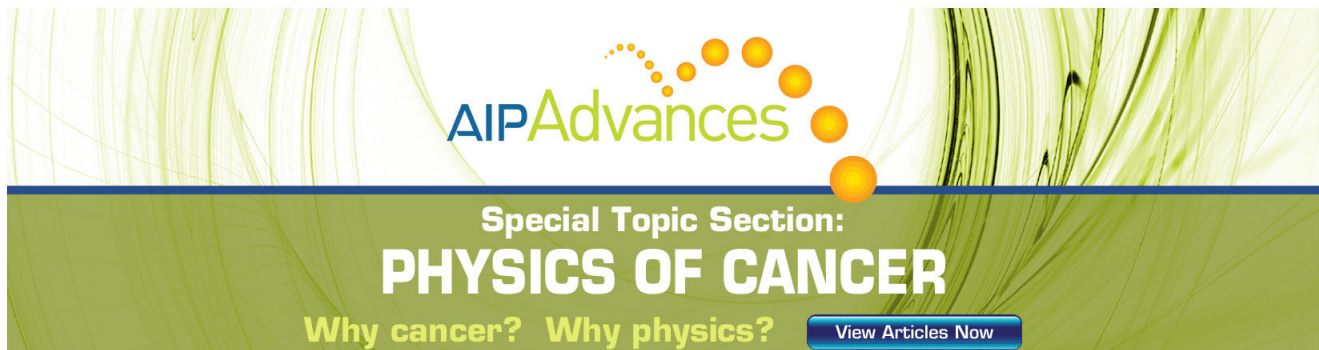
Journal Homepage: <http://pop.aip.org/>

Journal Information: http://pop.aip.org/about/about_the_journal

Top downloads: http://pop.aip.org/features/most_downloaded

Information for Authors: <http://pop.aip.org/authors>

ADVERTISEMENT



AIP Advances

Special Topic Section:
PHYSICS OF CANCER

Why cancer? Why physics? [View Articles Now](#)

Damping of relativistic electron beams by synchrotron radiation

F. Andersson^{a)}

Department of Electromagnetics, Chalmers University of Technology and EURATOM-VR Association, Göteborg, Sweden

P. Helander

EURATOM/UKAEA Fusion Association, Culham Science Centre, Abingdon, Oxfordshire OX14 3DB, United Kingdom

L.-G. Eriksson

Association EURATOM-CEA sur la Fusion, CEA Cadarache, St. Paul lez Durance, France

(Received 19 February 2001; accepted 21 September 2001)

Relativistic electrons emit synchrotron radiation due to their gyro- and guiding-center motions in a curved magnetic field. In this article, the kinetic theory of relativistic electron beams is developed to account for radiation reaction by including the Abraham–Lorentz reaction force in the kinetic equation. As an application of this theory, the dynamics of runaway electrons is examined and a steady-state solution is constructed describing a balance between acceleration by the electric field, pitch-angle scattering, and radiation reaction. Furthermore, it is found that a beam of relativistic electrons can be slowed down by the combined effects of pitch-angle scattering and radiation reaction. This damping can be more efficient than ordinary collisional drag, and appears to explain the decay of post-disruption runaway currents in the Joint European Torus (JET) [R. D. Gill, *Nucl. Fusion* **33**, 1613 (1993)]. © 2001 American Institute of Physics. [DOI: 10.1063/1.1418242]

I. INTRODUCTION

An electron beam passing through a plasma is damped by collisional friction against the plasma ions and electrons. If the plasma is immersed in a magnetic field, so that the electrons execute gyro-motion, the beam can also be damped by emission of synchrotron radiation, which gives rise to a reaction force on the beam electrons. This mechanism is operative even if the beam is parallel to the field since collisional scattering causes individual electrons to acquire perpendicular momentum, leading to gyro-motion and synchrotron radiation emission. The present article is devoted to the kinetic theory of these processes. We derive the kinetic equation for relativistic electrons experiencing Coulomb collisions and synchrotron radiation emission, and solve this equation in physically interesting limits, enabling us to calculate the damping of electron beam currents by these effects.

Although we keep the analysis as general as possible, we apply the theory to a more specific problem: the dynamics of runaway electrons in tokamaks. As is well known, the presence of an electric field in a plasma (such as the induced field in a tokamak) can lead to production of a high-energy “runaway” electron population due to the fact that the friction force decreases with increasing velocity for fast electrons.¹ If the plasma density is low, runaway production can occur in normal, nondisruptive, tokamak operation due to the Ohmic electric field. By constructing a steady-state solution to the kinetic equation where the runaway production is balanced by collisional and radiative damping, we are able to calculate the distribution function of fast electrons in such discharges.

Runaway production is particularly virulent during tokamak disruptions, where very large electric fields can be induced. In the Joint European Torus (JET),² a large (~ 1 MA) runaway current sometimes persists long after a disruption, showing a smooth decay on a time scale of 1 or 2 s. This decay cannot be explained by collisional drag alone since an accelerating electric field is induced during the decay which almost balances the drag, thus leading to a very slow net damping. It has been proposed that the decay could instead be caused by emission of synchrotron radiation.² Our kinetic analysis allows a quantitative assessment of this hypothesis, and suggests that the observed damping is broadly consistent with the theoretical expectation.

The article is organized as follows. In Sec. II the reaction of synchrotron radiation emission on the motion of a single electron is calculated. In the next section this effect is included in the kinetic equation for strongly relativistic electron beams. This equation is then solved in the following two sections, where the steady-state solution is constructed in Sec. IV, and the damping of an initially collimated beam is calculated in Sec. V. To complement these approximate, analytical solutions, numerical Monte Carlo simulations are presented in the following section. These results are then compared in Sec. VII with measurements of postdisruption currents in JET, and our conclusions are summarized in Sec. VIII.

II. LOSS OF ELECTRON MOMENTUM DUE TO RADIATION

In this section we calculate the average reaction force on a relativistic electron caused by its emission of synchrotron radiation. The velocity vector of a beam electron parallel to

^{a)}Electronic mail: fredrik.andersson@elmagn.chalmers.se

the magnetic field need only be scattered slightly to acquire a Larmor rotation that can lead to substantial synchrotron radiation. Since the radiation from a relativistic particle is emitted in a cone centered around its velocity vector, the reaction force is mainly in the direction parallel to the magnetic field although it is the perpendicular motion that causes the radiation. The Abraham–Lorentz reaction force is,³

$$\mathbf{K} = \frac{q^2 \gamma^2}{6 \pi \epsilon_0 c^3} \left[\ddot{\mathbf{v}} + \frac{3 \gamma^2}{c^2} (\mathbf{v} \cdot \dot{\mathbf{v}}) \dot{\mathbf{v}} + \frac{\gamma^2}{c^2} \left(\mathbf{v} \cdot \ddot{\mathbf{v}} + \frac{3 \gamma^2}{c^2} (\mathbf{v} \cdot \dot{\mathbf{v}})^2 \right) \mathbf{v} \right], \quad (1)$$

where \mathbf{v} is the electron velocity vector and $\gamma = (1 - (v/c)^2)^{-1/2}$ is the relativistic mass factor. The time average $\langle \dots \rangle$ of the radiated power from an accelerated electron for which $\mathbf{v} \cdot \dot{\mathbf{v}} = 0$ thus becomes

$$-\langle \mathbf{K} \cdot \mathbf{v} \rangle = \frac{q^2 \gamma^4}{6 \pi \epsilon_0 c^3} |\dot{\mathbf{v}}|^2.$$

Writing the electron position vector as $\mathbf{r} = \mathbf{R} + \boldsymbol{\rho}$, where \mathbf{R} represents the location of the gyro-center and $\boldsymbol{\rho}$ the gyromotion, gives

$$|\dot{\mathbf{v}}|^2 = |\dot{\boldsymbol{\rho}}|^2 + |\ddot{\mathbf{R}}|^2 + 2\ddot{\mathbf{R}} \cdot \dot{\boldsymbol{\rho}}, \quad (2)$$

where we assume that the Larmor radius is small, $\rho \ll R$. By taking the time average of this expression and introducing the transit frequency $\omega_t = v_{\parallel}/R$, where R is the average magnetic field radius of curvature and the gyro-frequency $\Omega = eB/\gamma m_e$, we are able to estimate the relative magnitude of the terms. Since $\langle |\ddot{\mathbf{R}}|^2 \rangle = (\omega_t^2 R)^2$ and $\langle |\dot{\boldsymbol{\rho}}|^2 \rangle = (\Omega^2 \rho)^2$, these become

$$\frac{|\ddot{\mathbf{R}}|^2}{|\dot{\boldsymbol{\rho}}|^2} = \left(\frac{v_{\parallel}^2 \rho}{v_{\perp}^2 R} \right)^2,$$

$$\frac{\langle \ddot{\mathbf{R}} \cdot \dot{\boldsymbol{\rho}} \rangle}{\langle |\ddot{\mathbf{R}}|^2 \rangle} = \frac{\langle (d^4 \mathbf{R}/dt^4) \cdot \boldsymbol{\rho} \rangle}{\langle |\ddot{\mathbf{R}}|^2 \rangle} \sim \frac{\rho}{R} \ll 1.$$

It is clear that the curvature of the magnetic field only causes a small contribution to the reaction force unless v_{\perp}/v_{\parallel} is very small. The subscripts \perp and \parallel indicate directions perpendicular and parallel to the magnetic field, respectively.

The energy of the particle is $\mathcal{E} = \gamma m_e c^2 = m_e c^2 \sqrt{1+p^2}$ where $\mathbf{p} = \gamma \mathbf{v}/c$ is the normalized momentum, and the momentum loss can be calculated from the relation $\dot{\mathcal{E}} = \mathbf{K} \cdot \mathbf{v} = m_e c^2 p \dot{p}/\gamma$,

$$\langle \dot{p} \rangle = \left\langle \frac{\gamma \dot{\mathcal{E}}}{m_e c^2 p} \right\rangle = - \frac{q^2 \gamma^5}{6 \pi \epsilon_0 m_e c^5} \frac{\langle |\dot{\mathbf{v}}|^2 \rangle}{p}.$$

When $\rho \ll R$ the average rate of change of momentum becomes

$$\left\langle \frac{dp}{dt} \right\rangle_{\text{rad}} = - \frac{\sqrt{1+p^2}}{\tau_r} \left(p_{\perp}^2 + \frac{\rho_0^2}{R^2} p_{\parallel}^4 \right), \quad (3)$$

where $\tau_r = 6 \pi \epsilon_0 (m_e c)^3 / e^4 B^2$ is the radiation time scale, and $\rho_0 = m_e c / eB$. We observe that $\dot{p}_{\parallel} = v v_{\parallel} \dot{p}/c^2$, and by defining the pitch-angle variable $\xi \equiv p_{\parallel}/p = \cos \theta$ we obtain

$$\frac{\dot{\xi}}{\xi} = \frac{\dot{p}_{\parallel}}{p_{\parallel}} - \frac{\dot{p}}{p} = \frac{\dot{p}}{p} \left(\frac{v^2}{c^2} - 1 \right) = - \frac{1}{\gamma^2} \frac{\dot{p}}{p}.$$

For a beam electron ξ is very close to unity, and its average rate of change thus becomes

$$\left\langle \frac{d\xi}{dt} \right\rangle_{\text{rad}} = \frac{1}{\gamma^2 p} \frac{\sqrt{1+p^2}}{\tau_r} \left(p_{\perp}^2 + \frac{\rho_0^2}{R^2} p_{\parallel}^4 \right). \quad (4)$$

Equations (3) and (4) summarize the average effect of radiation reaction on beam electrons.

III. KINETIC EQUATION FOR RELATIVISTIC ELECTRONS

The kinetics of the distribution function of superthermal electrons is governed by the relativistic Fokker–Planck equation,^{4,5}

$$\begin{aligned} \frac{\partial f}{\partial t} + \frac{-eE_{\parallel}}{m_e c} \left(\xi \frac{\partial f}{\partial p} + \frac{1-\xi^2}{p} \frac{\partial f}{\partial \xi} \right) - (1-\xi^2) \frac{cp}{\sqrt{1+p^2}} \\ \times \frac{\nabla_{\parallel} B}{2B} \frac{\partial f}{\partial \xi} + \left\langle \frac{dp}{dt} \right\rangle_{\text{rad}} \frac{\partial f}{\partial p} + \left\langle \frac{d\xi}{dt} \right\rangle_{\text{rad}} \frac{\partial f}{\partial \xi} \\ = \frac{1}{\tau} \left[\frac{1}{p^2} \frac{\partial}{\partial p} (1+p^2) f + \frac{(1+Z)}{2} \right. \\ \left. \times \frac{\sqrt{1+p^2}}{p^3} \frac{\partial}{\partial \xi} (1-\xi^2) \frac{\partial f}{\partial \xi} \right], \quad (5) \end{aligned}$$

where $\tau = 4 \pi \epsilon_0^2 m_e^2 c^3 / n_e e^4 \ln \Lambda$ is the collision time for relativistic electrons, n_e is the plasma electron density, and Z is the effective ion charge. This equation describes the effects of accelerating electric field, mirror force, radiation reaction, collisional drag and pitch-angle scattering. For strongly relativistic runaway electrons with $p \gg 1$ and $1-\xi \ll 1$, it is convenient to change the independent variables to $(p_{\parallel}, p_{\perp})$, so that acceleration by the electric field is described by

$$\frac{-eE_{\parallel}}{m_e c} \left(\xi \frac{\partial f}{\partial p} + \frac{1-\xi^2}{p} \frac{\partial f}{\partial \xi} \right) = \frac{-eE_{\parallel}}{m_e c} \frac{\partial f}{\partial p_{\parallel}},$$

and the radiation reaction terms become

$$\left\langle \frac{dp}{dt} \right\rangle_{\text{rad}} \frac{\partial f}{\partial p} + \left\langle \frac{d\xi}{dt} \right\rangle_{\text{rad}} \frac{\partial f}{\partial \xi} \approx - \frac{1}{\tau_r} \left(p_{\perp}^2 + \frac{\rho_0^2}{R^2} p_{\parallel}^4 \right) \frac{\partial f}{\partial p_{\parallel}},$$

where we have used Eqs. (3) and (4). When expressed in these variables, the slowing down operator can be approximated as

$$\begin{aligned} \frac{1}{p^2} \frac{\partial}{\partial p} (1+p^2) f = \frac{\partial}{\partial p_{\parallel}} \left(\left(1 + \frac{1}{p^2} \right) \frac{p_{\parallel}}{p} f \right) \\ + \frac{1}{p_{\perp}} \frac{\partial}{\partial p_{\perp}} \left(\left(1 + \frac{1}{p^2} \right) \frac{p_{\perp}^2}{p} f \right) \approx \frac{\partial f}{\partial p_{\parallel}}. \end{aligned}$$

This approximation is valid when $p_{\perp} \ll p_{\parallel}$ and $f p_{\perp}/p \ll \partial f/\partial p_{\perp}$ since then the discarded terms are much smaller than that retained from pitch-angle scattering, which becomes

$$\begin{aligned} \frac{\partial}{\partial \xi} (1 - \xi^2) \frac{\partial f}{\partial \xi} &\approx p_{\parallel} \frac{p}{p_{\perp}} \frac{\partial}{\partial p_{\perp}} p_{\parallel} \frac{p_{\perp}}{p} \frac{\partial f}{\partial p_{\perp}} \\ &\approx p^2 \frac{1}{p_{\perp}} \frac{\partial}{\partial p_{\perp}} p_{\perp} \frac{\partial f}{\partial p_{\perp}}, \end{aligned}$$

if terms of order $O(fE/p_{\parallel})$ are neglected. This approximation can be justified *a posteriori*.

The kinetic equation for a beam-like ($p_{\perp} \ll p_{\parallel}$) distribution of strongly relativistic electrons experiencing an electric field, Coulomb collisions and synchrotron radiation reaction thus becomes

$$\begin{aligned} \tau \frac{\partial f}{\partial t} + \left(E - 1 - \sigma \left(p_{\perp}^2 + \frac{\rho_0^2}{R^2} p_{\parallel}^4 \right) \right) \frac{\partial f}{\partial p_{\parallel}} \\ = \frac{1+Z}{2p_{\perp}} \frac{\partial}{\partial p_{\perp}} \left(p_{\perp} \frac{\partial f}{\partial p_{\perp}} \right), \end{aligned} \quad (6)$$

where $\sigma = \tau/\tau_r$, $E = |E_{\parallel}|/E_c = |E_{\parallel}|e\tau/m_e c$, and we have assumed E_{\parallel} to be negative. E_c is the electric field corresponding to the friction on strongly relativistic electrons. Thus, E_c is the critical electric field in the sense that electron runaway is possible when $E = |E_{\parallel}|/E_c > 1$, but not when $E < 1$.⁴ E_c should not be confused with the Dreicer field $E_D = (m_e c^2/T_e) E_c$, which is much larger than E_c and corresponds to the friction on thermal electrons.^{1,6} When $|E_{\parallel}| > E_D$, the entire electron population runs away, but in practice E_D is so large that this rarely occurs in tokamaks.

IV. STEADY-STATE DISTRIBUTION

When a tokamak is operated at low density, the Ohmic electric field used to drive plasma current can be large in the sense that $E > 1$, so that small amounts of runaway electrons are produced. Traditionally, the problem that has attracted most attention in runaway theory is that of calculating the rate at which the number of runaway electrons increases.⁴⁻⁷ In these calculations the runaway distribution never reaches a steady state. Our inclusion of radiation reaction in the kinetic equation allows us to consider the saturation of the runaway process and to calculate the distribution function of fast electrons in tokamak discharges with $E > 1$. Thus, in this section we construct steady-state solutions to the kinetic equation (6) arising as a balance between acceleration by the electric field, pitch-angle scattering, and radiation reaction. Equation (6) is only valid in the high-energy region $p_{\perp}/p \ll 1 \ll p$. The runaway mechanism feeds electrons from lower energies into this region, thus providing a boundary condition at small p_{\parallel} , where the distribution function should be proportional to $\delta(p_{\perp})$, reflecting the circumstance that runaway electrons are generated with small perpendicular momenta.

As we shall discuss later, there are two mechanisms capable of generating runaway electrons, primary and secondary generation. The results presented in this section do not depend on which of these is operative since we only solve the kinetic equation in the high-energy region where energy diffusion, which is responsible for primary generation, and the Møller scattering source term causing secondary generation (see below) are both small. The source of runaways instead enters as a boundary condition.

As we shall also see, the character of the steady-state solution to Eq. (6) depends on the curvature of the magnetic field, which controls the relative importance of the two terms in the energy loss rate (3). Accordingly, we shall consider three different limits: those of a straight, a weakly curved, and a strongly curved magnetic field.

A. Straight magnetic field

The simplest situation occurs when the radius of curvature R is infinite, so that the energy loss is entirely due to gyro-motion. Thus neglecting the term proportional to p_{\parallel}^4 in Eq. (6) gives

$$(E - 1 - \sigma p_{\perp}^2) \frac{\partial f}{\partial p_{\parallel}} = \frac{1+Z}{2p_{\perp}} \frac{\partial}{\partial p_{\perp}} \left(p_{\perp} \frac{\partial f}{\partial p_{\perp}} \right). \quad (7)$$

This is a so-called two-way diffusion equation since $h(p_{\perp}) \equiv 2p_{\perp}(E - 1 - \sigma p_{\perp}^2)/(1+Z)$ changes sign in the interval of interest.⁸ Such equations have the general form

$$h(p_{\perp}) \frac{\partial f(p_{\parallel}, p_{\perp})}{\partial p_{\parallel}} = \frac{\partial}{\partial p_{\perp}} D(p_{\perp}) \frac{\partial f(p_{\parallel}, p_{\perp})}{\partial p_{\perp}}, \quad (8)$$

with independent variables in the domain $a < p_{\perp} < b$, $0 < p_{\parallel} < L$ and with $D(p_{\perp})$ assumed positive. If $h(p_{\perp})$ had remained positive throughout the interval $a < p_{\perp} < b$, then Eq. (8) would represent the usual type of diffusion equation, which is well posed when initial conditions are given at $p_{\parallel} = 0$ and boundary conditions are given at $p_{\perp} = a$ and $p_{\perp} = b$. (The variable p_{\parallel} plays the role of time.) However, $h(p_{\perp})$ changes sign in the interval (a, b) and Eq. (8) describes diffusion with a variable sense of time. When $h(p_{\perp})$ is positive diffusion takes place with increasing p_{\parallel} , and when $h(p_{\perp})$ is negative diffusion occurs with decreasing p_{\parallel} . This type of equation is well posed only when initial conditions are given where $h(p_{\perp})$ is positive and final conditions are given where $h(p_{\perp})$ is negative. That is, the usual initial conditions are replaced by a combination of initial and final conditions,⁸

$$f(0, p_{\perp}) = f_+(p_{\perp}), \quad \text{where } h(p_{\perp}) > 0,$$

$$f(L, p_{\perp}) = f_-(p_{\perp}), \quad \text{where } h(p_{\perp}) < 0.$$

Physically, this means that boundary conditions are imposed where particles flow *into* the domain under consideration. Solving this type of equation by separation of variables results in an eigenvalue problem

$$\frac{\partial}{\partial p_{\perp}} D(p_{\perp}) \frac{\partial g_{\lambda}}{\partial p_{\perp}} = \lambda h(p_{\perp}) g_{\lambda}(p_{\perp}),$$

which cannot be analyzed by usual Sturm–Liouville theory. Since $h(p_{\perp})$ vanishes in the interval (a, b) , the eigenfunctions g_{λ} do not necessarily form a complete set. However, Fisch and Kruskal⁸ proved completeness on the interval (a, b) of these eigenfunctions when they are supplemented by the “diffusion solution” $f(p_{\parallel}, p_{\perp}) = p_{\parallel} - g(p_{\perp})$, where $g(p_{\perp})$ satisfies

$$\frac{\partial}{\partial p_{\perp}} D(p_{\perp}) \frac{\partial g}{\partial p_{\perp}} + h(p_{\perp}) = 0.$$

It was later shown by Beals⁹ that the eigenfunctions g_λ having negative eigenvalues form a complete set on the part of the domain where initial conditions are imposed, while those with positive eigenvalues are complete where final conditions are imposed. Beals also gives an iterative procedure for constructing solutions on finite intervals, based on the partial-range completeness result. Since the eigenfunctions do not have the usual orthogonality property on these intervals, this procedure is nontrivial.

We now proceed to solve the kinetic equation (7) in two opposite limits, of large and small values of p_\parallel . The boundary and initial/final conditions are

$$\begin{aligned} f(p_\perp \rightarrow \infty) &= 0, \\ f(p_\parallel \rightarrow 0, h(p_\perp) > 0) &\propto \delta(p_\perp), \\ f(p_\parallel \rightarrow \infty) &= 0, \end{aligned} \tag{9}$$

since we expect runaways to be generated with small p_\perp , so that the distribution function f is concentrated at small p_\perp when p_\parallel is small. Because of this condition, radiation can be ignored altogether for sufficiently small p_\parallel , in which case the kinetic equation (7) reduces to a simple diffusion equation with a well-known solution,^{4,6,7}

$$f(p_\parallel, p_\perp) = C_1 \frac{1}{p_\parallel} \exp\left(-\frac{E-1}{2(1+Z)} \frac{p_\perp^2}{p_\parallel}\right), \tag{10}$$

where C_1 is an arbitrary constant. Our neglect of the radiation reaction term is justified if $\sigma p_\perp^2 \ll E-1$, which is true for most electrons if $p_\parallel \ll (E-1)^2/2\sigma(1+Z)$.

To find the distribution of electrons with larger momenta, we separate variables in the kinetic equation (7) as outlined earlier. By introducing $p_\perp^2 = p_x^2 + p_y^2$, $p_z = p_\parallel(1+Z)/2(E-1)$, and seeking a solution of the form $f(p_x, p_y, p_z) = X(p_x)Y(p_y)Z(p_z)$, the kinetic equation becomes

$$\frac{1}{Z} \frac{dZ}{dp_z} = \left(1 - \frac{\sigma}{E-1} (p_x^2 + p_y^2)\right)^{-1} \left(\frac{1}{X} \frac{d^2X}{dp_x^2} + \frac{1}{Y} \frac{d^2Y}{dp_y^2}\right) = -\zeta.$$

It is clear that $Z(p_z) = \exp(-\zeta p_z)$, and

$$\begin{aligned} \frac{d^2X}{dp_x^2} + \zeta \left(\eta - \frac{\sigma}{E-1} p_x^2\right) X &= 0, \\ \frac{d^2Y}{dp_y^2} + \zeta \left(\nu - \frac{\sigma}{E-1} p_y^2\right) Y &= 0, \end{aligned}$$

where $\eta + \nu = 1$. This type of eigenvalue problem is equivalent to the Schrödinger equation for a one-dimensional harmonic oscillator whose eigenfunctions involve Hermite polynomials H_n . The eigenfunctions and eigenvalues are

$$\begin{aligned} X_k(p_x) &= \exp\left(-\frac{\sqrt{\zeta \sigma/(E-1)}}{2} p_x^2\right) H_k\left(p_x \left(\frac{\zeta \sigma}{E-1}\right)^{1/4}\right), \\ \eta_k &= \sqrt{\frac{\sigma/(E-1)}{\zeta}} (2k+1), \quad k=0,1,\dots, \end{aligned}$$

and analogously for $Y_l(p_y)$ and ν_l . The eigenfunctions and eigenvalues to Eq. (7) thus become

$$\begin{aligned} f_{kl}(p_\parallel, p_x, p_y) &= \exp\left(-\gamma_{kl} \frac{(1+Z)}{2\sigma} p_\parallel - \frac{\sqrt{\gamma_{kl}}}{2} (p_x^2 + p_y^2)\right) \\ &\quad \times H_k(p_x \gamma_{kl}^{1/4}) H_l(p_y \gamma_{kl}^{1/4}), \\ \gamma_{kl} &= \zeta_{kl} \frac{\sigma}{E-1} = \left(\frac{2\sigma}{E-1}\right)^2 (k+l+1)^2, \quad k, l=0,1,\dots \end{aligned} \tag{11}$$

Since the eigenfunctions form a complete set (the diffusion solution does not contribute since it is linear in p_\parallel), the boundary condition can be satisfied by a sum

$$f = \sum_{k=0}^{\infty} \sum_{l=0}^{\infty} c_{kl} f_{kl}.$$

However, as has already been mentioned, these eigenfunctions, although complete, do not form an orthogonal set and it is therefore difficult to use them to represent an arbitrary function, even for our simple delta function boundary condition. Instead, we observe that for large p_\parallel the dominant behavior of f is found from the eigenfunction with the lowest eigenvalue since the eigenfunctions decay exponentially, $f_{kl} \propto \exp(-\gamma_{kl}(1+Z)p_\parallel/2\sigma)$.

In the region $p_\parallel \gg (E-1)^2/2\sigma(1+Z)$ the solution to the kinetic equation (7) can therefore be written as

$$f(p_\parallel, p_\perp) = c_{00} f_{00} = C_2 \exp\left(-\frac{\sigma}{E-1} \left(\frac{2(1+Z)}{E-1} p_\parallel + p_\perp^2\right)\right), \tag{12}$$

where C_2 is an undetermined constant.

The approximations made in reaching the kinetic equation (6) can now be justified by estimating the magnitude of the discarded terms. One finds that the terms retained in Eq. (6) are all of order $O(f\sigma/E)$, while the largest term among those discarded is $\tau \dot{p}_\perp \partial f / \partial p_\perp$ which is of order $O(fE/p_\parallel)$ if $\gamma \gg 1$. Since $p_\parallel \gg (E-1)^2/2\sigma(1+Z)$ we find an upper limit to the latter term, $O(fE/p_\parallel) \ll O(f\sigma/E)$, which justifies its neglect. In these estimates we used the fact that in the range of validity of solution (12), $p_\perp^2 = O(E/\sigma)$, $\gamma^2 = O(p_\parallel^2)$ for large p , and $1 - \xi \approx p_\perp^2/2p_\parallel^2 \ll 1$.

B. Weakly curved magnetic field

In a curved magnetic field, not only gyro-motion but also guiding-center motion gives rise to radiation. By introducing the normalized variables $\tilde{p}_\parallel = p_\parallel/p_{\parallel 0}$ and $\tilde{p}_\perp = p_\perp/p_{\perp 0}$, with $p_{\parallel 0} = 2(E-1)^2/\sigma(1+Z)$ and $p_{\perp 0}^2 = (E-1)/\sigma$, we can write the kinetic equation (6) as

$$(1 - \tilde{p}_\perp^2 - s \tilde{p}_\parallel^4) \frac{\partial f}{\partial \tilde{p}_\parallel} = \frac{1}{\tilde{p}_\perp} \frac{\partial}{\partial \tilde{p}_\perp} \tilde{p}_\perp \frac{\partial f}{\partial \tilde{p}_\perp}, \tag{13}$$

where the parameter

$$s \equiv \frac{\rho_0^2}{R^2} \frac{p_{\parallel 0}^4}{p_{\perp 0}^2} = \left(\frac{2}{1+Z}\right)^4 \frac{(E-1)^7}{\sigma^3} \left(\frac{\rho_0}{R}\right)^2 \tag{14}$$

governs the relative importance of the two radiation terms.

There is an interesting qualitative difference between the radiation reaction caused by these two terms. Since we have assumed $E > 1$, s is positive and $1 - \tilde{p}_\perp^2 - s \tilde{p}_\parallel^4$ can thus only be positive if $\tilde{p}_\parallel < s^{-1/4}$, which implies that f vanishes for

sufficiently large \tilde{p}_\parallel . The physical reason for this is that electrons cannot be accelerated beyond the synchrotron limit

$$p_\parallel < \left(\frac{R}{\rho_0}\right)^{1/2} \left(\frac{E-1}{\sigma}\right)^{1/4}, \tag{15}$$

at which the radiation reaction force associated with magnetic field curvature equals the force from the electric field. Thus, while electrons in a straight field can reach arbitrarily high energies, there is an absolute upper limit to the attainable energy of electrons in a curved magnetic field.

If $s \ll 1$, synchrotron radiation produced by gyro-motion is more important than that from curved guiding-center motion for most particles. The analysis presented in the previous subsection then applies for most of the fast electrons. However, it is clear that sufficiently fast electrons will always suffer strong energy losses caused by magnetic field curvature, since this term is proportional to p_\parallel^4 . Thus, to calculate the distribution of electrons at the highest end of the energy spectrum it is necessary to include this term in the analysis even if s is small. This is the subject of the present subsection, while the opposite limit, $s \gg 1$, is treated in the next section.

In order to solve the kinetic equation (13) in the limit $s \ll 1$, we introduce

$$\begin{aligned} x(\tilde{p}_\parallel) &\equiv \int_0^{\tilde{p}_\parallel} \frac{d\tilde{p}'_\parallel}{(1-s\tilde{p}'_\parallel{}^4)^2} \\ &= \frac{1}{4} \frac{\tilde{p}_\parallel}{1-s\tilde{p}_\parallel^4} + \frac{3}{16} s^{-1/4} \ln\left(\frac{1+\tilde{p}_\parallel s^{1/4}}{1-\tilde{p}_\parallel s^{1/4}}\right) \\ &\quad + \frac{3}{8} s^{-1/4} \arctan(\tilde{p}_\parallel s^{1/4}), \end{aligned}$$

so that $1-s\tilde{p}_\parallel^4 \rightarrow 0$ and $x \rightarrow \infty$ at the synchrotron limit, $\tilde{p}_\parallel \rightarrow s^{-1/4}$. Equation (13) thus becomes

$$\left(1 - \frac{\tilde{p}_\perp^2}{1-s\tilde{p}_\parallel^4}\right) \frac{\partial f}{\partial x} = \frac{1-s\tilde{p}_\parallel^4}{\tilde{p}_\perp} \frac{\partial}{\partial \tilde{p}_\perp} \tilde{p}_\perp \frac{\partial f}{\partial \tilde{p}_\perp}, \tag{16}$$

which suggests a change of variables $(x, \tilde{p}_\perp) \rightarrow (x, y)$ where $y \equiv \tilde{p}_\perp / \sqrt{1-s\tilde{p}_\parallel^4(x)}$, so that

$$\frac{\partial}{\partial \tilde{p}_\perp} \rightarrow \frac{1}{\sqrt{1-s\tilde{p}_\parallel^4}} \frac{\partial}{\partial y}$$

and

$$\frac{\partial}{\partial x} \rightarrow \frac{\partial}{\partial x} + 2s\tilde{p}_\parallel^3 y \frac{\partial}{\partial y}, \tag{17}$$

where the second term in Eq. (17) is smaller than the first one if $y = O(1)$ and $2s\tilde{p}_\parallel^3 \ll 1$. Since $\tilde{p}_\parallel \leq s^{-1/4}$ this condition is automatically satisfied if $s^{1/4} \ll 1$. We thus obtain the two-way diffusion equation

$$(1-y^2) \frac{\partial f}{\partial x} = \frac{1}{y} \frac{\partial}{\partial y} y \frac{\partial f}{\partial y}, \tag{18}$$

which can be treated by the same method as used in the previous subsection. The eigenfunction corresponding to the lowest eigenvalue, and therefore representing the dominant behavior of f for large p_\parallel , is

$$f_{00}(x, y) = \exp(-4x - y^2). \tag{19}$$

This eigenfunction is dominant when $4x(\tilde{p}_\parallel) \gg 1$, which implies a lower bound on p_\parallel for the solution to be valid. The distribution function thus becomes

$$\begin{aligned} f(\tilde{p}_\parallel, \tilde{p}_\perp) &= C_3 \left(\frac{1-\tilde{p}_\parallel s^{1/4}}{1+\tilde{p}_\parallel s^{1/4}}\right)^{3/4} s^{-1/4} \exp\left(-\frac{1}{1-s\tilde{p}_\parallel^4}(\tilde{p}_\parallel + \tilde{p}_\perp^2)\right. \\ &\quad \left.- \frac{3}{2} s^{-1/4} \arctan(\tilde{p}_\parallel s^{1/4})\right), \end{aligned} \tag{20}$$

where C_3 is an undetermined constant. Since the synchrotron limit $\tilde{p}_\parallel \leq s^{-1/4}$ defines an upper bound on p_\parallel , we find that p_\parallel lies in the following region,

$$\frac{(E-1)^2}{2\sigma(1+Z)} \ll p_\parallel \leq \left(\frac{R}{\rho_0}\right)^{1/2} \left(\frac{E-1}{\sigma}\right)^{1/4}.$$

As long as p_\parallel is well below the synchrotron limit, so that $\tilde{p}_\parallel \ll s^{-1/4}$, the distribution function (19) coincides with that in a straight magnetic field (12) since then $x \approx \tilde{p}_\parallel$ and $y \approx p_\perp s^{1/2}$. When p_\parallel approaches the synchrotron limit, $\tilde{p}_\parallel \rightarrow s^{-1/4}$, the distribution function decays very rapidly since $x \rightarrow \infty$, and the electron beam becomes very narrow (in p_\perp) since $1-s\tilde{p}_\parallel^4 \rightarrow 0$.

C. Strongly curved magnetic field

We finally turn our attention to the limit $s \gg 1$ of a strongly curved magnetic field, where most synchrotron radiation is emitted as a consequence of guiding-center motion rather than gyro-motion. This limit is rarely realized under normal tokamak conditions but is presented here for completeness.

Since $\tilde{p}_\perp^2 \ll s\tilde{p}_\parallel^4$ when $s \gg 1$ this term can be neglected in the kinetic equation (13), and by introducing

$$\begin{aligned} x(\tilde{p}_\parallel) &\equiv \int_0^{\tilde{p}_\parallel} \frac{d\tilde{p}'_\parallel}{(1-s\tilde{p}'_\parallel{}^4)} \\ &= \frac{1}{4s^{1/4}} \left(2\arctan(\tilde{p}_\parallel s^{1/4}) + \ln\left(\frac{1+\tilde{p}_\parallel s^{1/4}}{1-\tilde{p}_\parallel s^{1/4}}\right)\right), \end{aligned}$$

so that $x \rightarrow \infty$ as $\tilde{p}_\parallel \rightarrow s^{-1/4}$, the equation becomes approximately

$$\frac{\partial f}{\partial x} = \frac{1}{\tilde{p}_\perp} \frac{\partial}{\partial \tilde{p}_\perp} \tilde{p}_\perp \frac{\partial f}{\partial \tilde{p}_\perp}, \tag{21}$$

which is a simple diffusion equation with the solution

$$f(x, \tilde{p}_\perp) = \frac{1}{x} \exp\left(-\frac{\tilde{p}_\perp^2}{4x}\right).$$

The solution to the kinetic equation (13) when $s \gg 1$ thus becomes

$$f(\tilde{p}_{\parallel}, \tilde{p}_{\perp}) = C_4 s^{1/4} \left(2 \arctan(\tilde{p}_{\parallel} s^{1/4}) + \ln \left(\frac{1 + \tilde{p}_{\parallel} s^{1/4}}{1 - \tilde{p}_{\parallel} s^{1/4}} \right) \right)^{-1} \\ \times \exp \left(-s^{1/4} \tilde{p}_{\perp}^2 \left(2 \arctan(\tilde{p}_{\parallel} s^{1/4}) \right. \right. \\ \left. \left. + \ln \left(\frac{1 + \tilde{p}_{\parallel} s^{1/4}}{1 - \tilde{p}_{\parallel} s^{1/4}} \right) \right)^{-1} \right), \quad (22)$$

where C_4 is an undetermined constant and p_{\parallel} is below the synchrotron limit (15). As this limit is approached from below, the distribution function decays rapidly while the width of the electron beam grows explosively. The width is ultimately limited at $\tilde{p}_{\perp}^2 \sim s \tilde{p}_{\parallel}^4 \sim s^{1/2}$, by the radiation term from gyro-motion, which we neglected in the approximate Eq. (21).

V. NUMERICAL SOLUTION OF THE KINETIC EQUATION

The orbit-averaged kinetic equation (5) is not separable and to find solutions to this full equation a numerical scheme is required. A Monte Carlo code, ARENA (Avalanche of Runaway Electrons, Numerical Analysis code),¹⁰ has been constructed for this purpose. It numerically solves Eq. (5) by representing a number of real particles by a so-called Monte Carlo particle which is periodically moved in phase space by the Monte Carlo operators. The code monitors a large number of such Monte Carlo particles when acted upon by operators representing collisions, accelerating electric field and radiation reaction. The code also includes the effect of secondary generation of runaway electrons by close collisions through the source term S given by Eq. (23) and added to the right-hand side of Eq. (5). In the ultrarelativistic region, $p \gg 1$, the runaway electrons are expected to move nearly parallel to the magnetic field, while newly born runaways are generated with a relatively small amount of momentum ($p \ll 1$) directed mainly in the perpendicular direction. In this approximation, calculating the source term by retaining only the leading order term in the quantum-mechanical Møller scattering formula¹¹ gives

$$S = \frac{n_r}{4\pi\tau \ln \Lambda} \delta(\xi - \xi_2) \frac{1}{p^2} \frac{\partial}{\partial p} \left(\frac{1}{1 - \sqrt{1 + p^2}} \right), \quad (23)$$

where $\xi_2 = p/(\sqrt{1 + p^2} + 1)$ and n_r is the density of runaway electrons. The accuracy of this approximation⁵ was confirmed numerically in Ref. 12.

To verify the accuracy of the Monte Carlo code ARENA an analytical solution of Eq. (6) is calculated in the following section. The code is put to full use in Sec. VII where it is compared to experimental measurements in JET.

VI. DAMPING OF RUNAWAY ELECTRON BEAMS

In this section we calculate the rate at which collisions and synchrotron radiation emission damp a relativistic electron beam. Thus, we seek solutions to the initial value problem given by Eq. (5) when the distribution function of fast electrons is specified at some initial time, $t=0$. One motivation for this is to try to explain the damping of postdisruption

currents in JET. As already mentioned in the Introduction, a large runaway current sometimes survives the disruption in JET and then decays on a time scale of 1 or 2 s. The results presented in this and the following section suggest that this decay is mainly caused by the emission of synchrotron radiation, while ordinary collisional friction only plays a minor role.

We begin by choosing an appropriate initial condition for the kinetic problem, which is given as the distribution function of runaway electrons immediately following the disruption. Of course, this distribution is not known in general, and its form depends on the mechanism by which the runaways were generated. In general, there are two ways of producing runaway electrons in a tokamak disruption: primary generation, where thermal electrons diffuse through the high-energy tail of the thermal electron population to increasingly higher energy;^{4,6,7} and secondary generation, where close collisions between existing runaways and thermal electrons knock the latter over the runaway threshold.^{5,10,13,14} The relative importance of these two mechanisms depends on the plasma current and the speed of the disruption. The secondary generation mechanism is only important in tokamaks with large enough current (such as JET), and produces runaways with a distribution function^{5,13}

$$f_0(p_{\parallel}, p_{\perp}) \propto \delta(p_{\perp}) e^{-p_{\parallel}/p_0}, \quad (24)$$

where $p_0 = 2 \ln \Lambda$. Although the generation mechanism is usually not known in JET, we shall take this to be our initial condition. There are at least two reasons for this: secondary generation probably occurs in at least some JET disruptions, and even if primary generation is the dominant mechanism this *ansatz* is still reasonable as it agrees broadly with the observed energy of runaways. The steady-state solutions found in the previous sections are not applicable to disruptions since the disruption time scale is much too short for any radiation effects to matter.

If collisional friction alone were responsible for the damping, one might be forgiven for thinking that this would occur on a time scale equal to $p_0 \tau$, which is typically about 2 s and thus consistent with the observations. However, it is important to realize that because of the large inductance of JET, the current decay must be accompanied by a sizable induced electric field. If the thickness of the current channel is neglected, this field is equal to

$$E = - \frac{l \tau}{I_A} \frac{dI}{dt}, \quad (25)$$

where I is the runaway current, $I_A = 4\pi m_e c / \mu_0 e = 0.017$ MA is the Alfvén current, and l is proportional to the plasma inductance, which we write as $L = \mu_0 l R / 2$. (In the ARENA code, the induced electric field is calculated more carefully from Maxwell's equations, and then varies across the current channel.) As we shall see later in this section, since typically $E > 1$ the electric field is large enough to reduce the current decay to a level far slower than what is observed. Friction therefore cannot be the principal agent for damping the runaway current.

Instead, we seek to explain the damping by the combined effect of Coulomb collisions and radiation reaction. To

do this to the necessary accuracy, a full solution of the kinetic equation (5) is required. This can only be found numerically and will be presented in the next section. In this section, we find an analytical solution to the simpler equation (6), which captures most of the physics correctly and can be used to benchmark the Monte Carlo code. However, unlike the situation in the previous sections, Eq. (6) is not strictly correct when the distribution function is time-dependent. The reason for this is that it neglects the contraction of the beam caused by radiation reaction, which is represented by a term $\tau \dot{p}_{\perp \text{rad}} \partial f / \partial p_{\perp}$. For the problem at hand, this term represents an ‘‘order unity effect’’ and is therefore kept in the numerical solution although it turns out not to affect the basic time scale of the current decay. By excluding it, we are able to solve analytically the kinetic problem (6), including the effect of the self-consistent induced electric field (25), and thus to verify the correctness of the code.

We now proceed to solve Eq. (6) by considering the case where the induced electric field is so small, $E < 1$, that it is no longer a two-way diffusion equation. Physically, this means that the electric field is too weak to generate new runaway electrons. Radiation reaction from magnetic field curvature can be neglected since the electric field for JET parameters makes the relevant parameter $s \ll 1$. It is possible to separate variables in Eq. (6), as in the case of a straight magnetic field, and its solution can thus be written as a superposition of eigenfunctions

$$f_{mn\lambda}(x, y, p_{\parallel}, t) = e^{-\lambda p_{\parallel} - (x^2 + y^2)\sqrt{\lambda}/2} \times H_m(x\lambda^{1/4})H_n(y\lambda^{1/4})T_{mn}(t, \lambda),$$

where $p_{\perp}^2 = [(1 + Z)/2\sigma]^{1/2}(x^2 + y^2)$ and H_n are Hermite polynomials. The functions $T_{mn}(t, \lambda)$ are determined by Eq. (25),

$$T_{mn}(t, \lambda) = C_5 \exp\left\{\left[\left(\frac{1 + Z}{2\tau\tau_r}\right)^{1/2} \gamma_{mn} - \frac{1}{\tau}\right] \lambda t - \frac{l}{I_A} \lambda I(t)\right\},$$

where C_5 is an integration constant and $\gamma_{mn} = -2(m + n + 1)/\sqrt{\lambda}$. The coefficients in the expansion of f in these eigenfunctions are determined by the initial condition (24). The distribution function thus becomes

$$f(x, y, p_{\parallel}, t) = \frac{e^{-p_{\parallel}/p_0}}{\pi T(0)\sqrt{p_0}} \times \sum_{j,k} \left(\frac{-1}{4}\right)^{j+k} \frac{1}{j!k!} e^{-(x^2 + y^2)/2\sqrt{p_0}} \times H_{2j}(xp_0^{1/4})H_{2k}(yp_0^{1/4})T_{2j,2k}(t, p_0^{-1}). \tag{26}$$

For simplicity, we assume that the radial current density is uniform in the runaway current channel which gives the current

$$I(t) = -e \int_0^a 2\pi r dr \int v_{\parallel} f d^3p.$$

By substituting Eq. (26) in this integral we obtain an implicit expression for the runaway current damping,

$$\begin{aligned} \frac{I(t)}{I_0} & \exp\left[\frac{l}{2I_A \ln \Lambda} (I(t) - I_0)\right] \\ & = \operatorname{sech}\left(t \sqrt{\frac{(1 + Z)}{\tau\tau_r \ln \Lambda}}\right) \exp\left(-\frac{t}{2\tau \ln \Lambda}\right). \end{aligned} \tag{27}$$

$I_0 = I(t = 0)$ is the runaway current immediately after the disruption. The exponential on the left describes the effect of the plasma inductance, which is to slow down the current decay by a factor of approximately

$$\alpha = \frac{II_0}{2I_A \ln \Lambda},$$

which is about 5 for typical conditions in JET ($I_0 \approx 1$ MA, $l \approx 2$). The sech factor on the right of Eq. (27) accounts for the effect of radiation damping, while the exponential it multiplies describes ordinary friction. Evidently, the time scale associated with radiative damping is

$$t_{\text{rad}} = \alpha \sqrt{\frac{\tau\tau_r \ln \Lambda}{1 + Z}},$$

while that of the friction is

$$t_{\text{fric}} = 2\alpha\tau \ln \Lambda.$$

Their ratio is equal to

$$\frac{t_{\text{fric}}}{t_{\text{rad}}} = \frac{3.2B_T}{\sqrt{(1 + Z)n_{19}}},$$

where $B_T = B/(1 \text{ T})$ and $n_{19} = n_e/(10^{19} \text{ m}^{-3})$, indicating that synchrotron radiation is more important than friction in JET since $B \approx 3 \text{ T}$, $Z = 1$ and $10^{19} \text{ m}^{-3} < n_e < 10^{20} \text{ m}^{-3}$ following a disruption. As has already been mentioned, because of the factor α caused by the large inductance of the JET plasma, the friction time scale t_{fric} is too long to explain the observed decay in JET. On the other hand, the time scale associated with damping by the emission of radiation, t_{rad} , agrees broadly with the observations.

It is not difficult to understand the physics behind the time scales t_{fric} and t_{rad} . The former simply reflects the fact that friction causes a particle to decelerate according to $dp/dt = -\tau$, so that it takes the time $p_0\tau$ to slow down a population of electrons with mean momentum $p_0 = 2 \ln \Lambda$. Multiplying this by the factor α by which plasma inductance resists the damping gives $t_{\text{fric}} = \alpha p_0\tau$. The time scale t_{rad} is associated with the combined action of pitch-angle scattering and radiation reaction. As indicated by the form of the scattering term in the kinetic equation (6), pitch-angle scattering makes an average electron acquire a perpendicular momentum p_{\perp} in the time

$$t_1 = \tau p_{\perp}^2 / (1 + Z).$$

According to Eq. (3), emission of radiation then causes the particle to slow down on a time scale

$$t_2 = \tau_r p_0 / p_{\perp}^2,$$

if the initial momentum was p_0 . Equating t_1 and t_2 finally gives the time scale $t_{\text{rad}} \sim \alpha t_1 = \alpha t_2$.

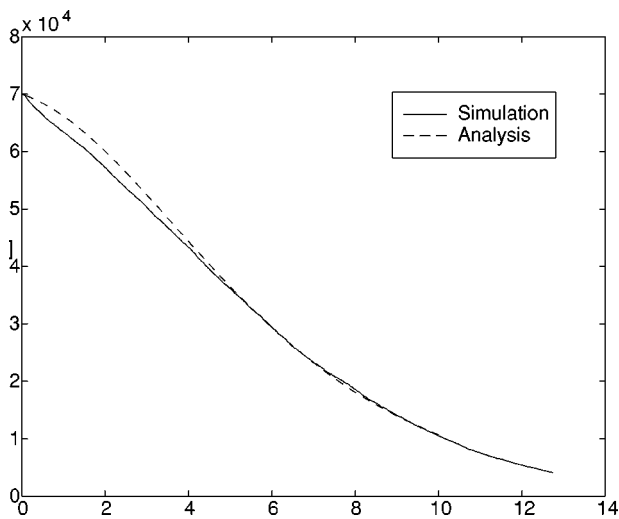


FIG. 1. Plasma current versus time. Comparison between analytical expression (27) and Monte Carlo simulation.

The existence of the analytical solution (27) gives a valuable opportunity to benchmark the ARENA code. If the latter is modified mildly so that it solves Eq. (6) rather than the full kinetic equation, it agrees nicely with Eq. (27) as shown in Fig. 1.

VII. EXPERIMENTAL COMPARISON

Disrupting discharges in JET showing a slow decay of the postdisruption plasma current have a generic behavior of exponential-like decay with a characteristic decay time of about 1 or 2 s. This plasma current is most likely exclusively carried by runaway electrons and its damping can be compared to the predictions from numerical simulations performed with the Monte Carlo code ARENA.

After a disruption there is usually a lack of reliable experimental measurements. Consequently, it is difficult to make detailed comparisons between experimental results and simulations of postdisruption runaway currents, and such a detailed comparison is beyond the scope of the present article. Nevertheless, it is of interest to see if the essential features of the runaway currents can be reproduced.

A typical example of a long-lived post-disruption plasma is discharge 14248, which has an exponential-like decay and an initial runaway current of about 0.6 MA (see Fig. 2). The disruption occurs shortly before $t = 50$ s, and the current then decays smoothly and approximately exponentially for about 8 s. As in many other discharges, immediately following the disruption the current exhibits some intermediate nonexponential behavior, in this case at $t \approx 50$ s. This indicates that there are other mechanisms involved at this early stage of the current damping, and we only endeavor to model the smooth current decay for $t > 50$ s.

Owing to the disruption, there are no reliable measurements of the effective ion charge or the electron density in the postdisruption phase in this discharge. It is likely that the density increases significantly following the disruption due to a large influx of neutral atoms and impurities,¹⁵ but it is difficult to know what the density and effective ion charge

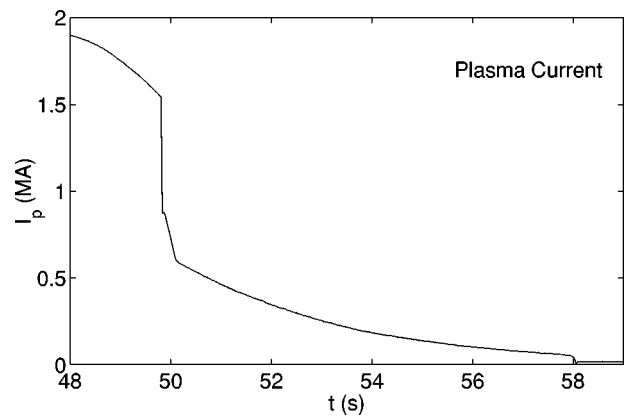


FIG. 2. Postdisruption plasma current in JET discharge 14248.

are long after the disruption. We have therefore carried out simulations with a range of different assumptions for these quantities. Three examples are shown in Fig. 3. In the first curve (a), the density and effective ion charge have been chosen so as to give good agreement with the observed current decay. The initial density (just after $t = 50$ s) was taken to be equal to six times its predisruption value, $n_{e0} = 1.4 \cdot 10^{19} \text{ m}^{-3}$, and then falling exponentially with a time constant of 5 s to one-fifth of the initial value. The effective ion charge was taken to be equal to 2 just after the disruption and then falling exponentially to 1 with a time constant of 0.5 s. Clearly these assumptions are fairly arbitrary, but appear quite realistic. The other two curves [(b) and (c)] show the current decay obtained with constant density and ion charge. The density was $n_e = 6n_{e0}$ and $n_e = n_{e0}$, respectively, while the effective ion charge was equal to unity in both cases. This lower choice of Z_{eff} makes the current decay more slowly than in case (a).

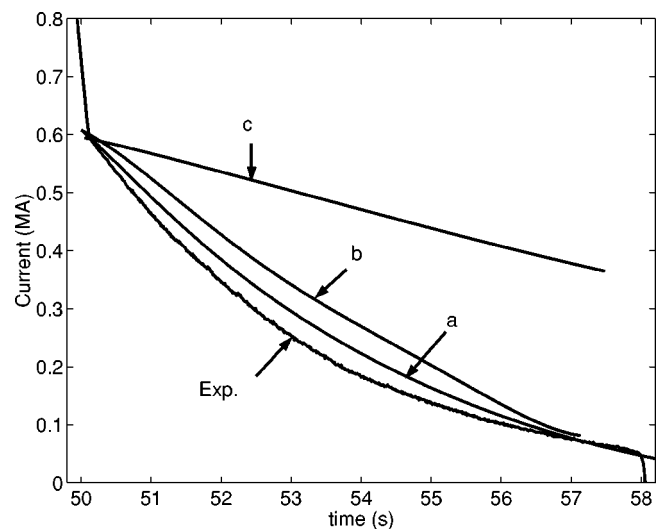


FIG. 3. Postdisruption plasma current in JET discharge 14248 and numerical results from the Monte Carlo code ARENA. Curve (a) shows a simulation where the density just after the disruption is six times higher than the predisruption value ($6n_{e0}$) and decreases exponentially, while the effective ion charge is initially equal to 2 and then decreases exponentially to 1. Curves (b) and (c) show simulations where the density is kept fixed at $6n_{e0}$ and n_{e0} , respectively, and $Z_{\text{eff}} = 1$.

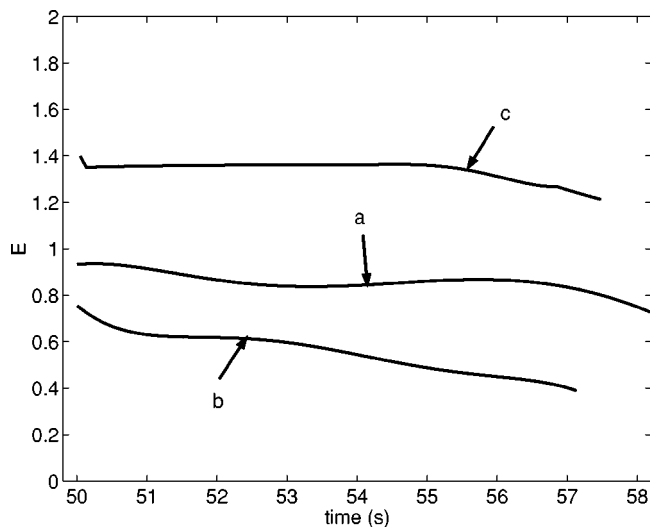


FIG. 4. Induced electric field normalized to the critical field, $E = |E_{\parallel}|/E_c$, for the three cases shown in Fig. 3.

These simulations suggest that the observed current decay can be explained by the emission of synchrotron radiation if the density increases significantly after the disruption [curves (a) and (b)]. Such an increase has also been conjectured for other reasons.^{15,16} If the density remains the same [curve (c)], synchrotron damping is less efficient and can only cause significant damping if the effective ion charge far exceeds unity. The reason for this is that if the density remains near its predisruption value, the critical electric field E_c is lower than that induced by the current decay, so that new runaways are created long after the disruption. This is illustrated by Fig. 4, which shows $E = |E_{\parallel}|/E_c$ in the three cases. Only in case (c) is $E > 1$, so that new secondaries are generated. Of course the current decay also depends to some extent on the assumed initial condition Eq. (24), which is the same in the three cases. At any rate, we may safely conclude that entirely “classical” mechanisms must be responsible for a large part of the damping, and there is no obvious need to invoke any beam-plasma instability to account for the observations.

VIII. CONCLUSIONS

In this article, we have developed a kinetic theory to describe the effects of Coulomb collisions and synchrotron radiation emission on relativistic electron beams in magne-

tized plasmas. Unlike collisional friction, the radiation reaction force increases with increasing energy and therefore always becomes important at sufficiently high energies, where it changes the electron dynamics in a qualitative way. For instance, if a constant electric field is applied to a magnetized plasma, synchrotron radiation reaction leads to saturation of the electron runaway mechanism, so that the runaway population stops increasing and instead reaches a steady state. In a tokamak, this may be important for establishing the kinetic equilibrium of runaway electrons in low-density, nondisrupting discharges, where the inductive electric field exceeds the critical one for electron runaway. It is unlikely to be of any significance in disruptions, which always occur on a time scale much shorter than the synchrotron radiation time scale. However, following a disruption, the runaway electron current can be damped by the combined action of Coulomb collisions and the radiation reaction force. This damping is surprisingly effective and is more efficient than ordinary collisional friction if the magnetic field is sufficiently strong. This is the case in JET, where this mechanism appears to be responsible for the observed damping of postdisruption runaway currents.

ACKNOWLEDGMENTS

This work was supported by the UK Dept of Trade and Industry, and by EURATOM under association contracts with France, Sweden, and the United Kingdom.

- ¹H. Dreicer, Phys. Rev. **115**, 238 (1959); **117**, 329 (1960).
- ²R. D. Gill, Nucl. Fusion **33**, 1613 (1993).
- ³W. Pauli, *Theory of Relativity* (Dover, New York, 1981).
- ⁴J. W. Connor and R. J. Hastie, Nucl. Fusion **15**, 415 (1975).
- ⁵M. N. Rosenbluth and S. V. Putvinski, Nucl. Fusion **37**, 1355 (1997).
- ⁶A. V. Gurevich, Sov. Phys. JETP **12**, 904 (1961).
- ⁷M. D. Kruskal and I. B. Bernstein, Princeton Plasma Physics Lab. Report No. MATT-Q-20, 174 (1962).
- ⁸N. J. Fisch and M. D. Kruskal, J. Math. Phys. **21**, 740 (1980).
- ⁹R. Beals, J. Math. Phys. **22**, 954 (1981).
- ¹⁰P. Helander, L.-G. Eriksson, and F. Andersson, Phys. Plasmas **7**, 4106 (2000).
- ¹¹C. Möller, Ann. Phys. (Leipzig) **14**, 531 (1932).
- ¹²S. C. Chiu, M. N. Rosenbluth, R. W. Harvey, and V. S. Chan, Nucl. Fusion **38**, 1711 (1998).
- ¹³R. Jayakumar, H. H. Fleischmann, and S. J. Zweben, Phys. Lett. A **172**, 447 (1993).
- ¹⁴H. H. Fleischmann and S. J. Zweben, “Evaluation of potential runaway generation in large-tokamak disruptions,” Technical Report, PPPL-2914 (1993), NTIS Order No.: DE93016724INZ.
- ¹⁵D. J. Ward and J. A. Wesson, Nucl. Fusion **32**, 1117 (1992).
- ¹⁶J. A. Wesson, R. D. Gill, and M. Hugon *et al.*, Nucl. Fusion **29**, 641 (1989).